

2D Airfoil Near-Wake Verification and Validation

ME 590-211

Author – Eric Adams

University of Kentucky

Department of Mechanical Engineering

December 1st, 2023

Abstract

This report meticulously explores meshing and solution development, engaging in a systematic comparison with NASA Turbulence Resource Center's published results for a 2D Airfoil Near Wake (2DANW) case as well as experimental results. The primary focus is on the validation and verification processes used to evaluate the model's robustness. Throughout this investigation, the report navigates the complexities of computational fluid dynamics (CFD), unraveling the detailed steps involved in crafting a nuanced CFD solution. Notably, the scrutiny applied to wake characteristics reveals certain methodological limitations, particularly in addressing the intricacies of the trailing edge and wake. Despite constraints—limited to 1048576 elements and a mere four parallel processes—the model captures air behavior near the airfoil, aligning with NASA's CFL3D and FUN3D models. The report dissects the nuances of mesh and solution development, highlighting a robust correlation with NASA's models near the airfoil but revealing less favorable outcomes in the airfoil wake. The discrepancies, especially at the trailing edge, emphasize the need for an improved meshing approach. Additionally, the report provides insights into the alignment of the solution with NASA's Spalart-Allmaras model, validated through meticulous grid independence assessments near the airfoil using $Y+$ values.

Table of Contents

Abstract.....	2
List of Figures	4
Nomenclature	5
Introduction	6
Model Description.....	9
Mesh.....	11
Mesh methodology.....	11
Mesh Description	12
Airfoil Surface Y+	16
Solution Methods	17
Verification.....	18
Validation.....	20
Results and Discussion.....	24
Results Overview	24
Issues with Meshing Approach.....	24
Additional Results.....	25
Conclusions	27
References.....	28
Appendix A – Hand Calculations for Problem Description.....	29
Appendix B – Modified Airfoil Grid.....	30

List of Figures

Figure 1: NASA Turbulence Modeling Resource 2D Airfoil Near-Wake Case	6
Figure 2: Ansys Fluent Viscous Model Options and SA Constants.....	9
Figure 3: Convergence Criteria of Y+ and Number of Elements.....	11
Figure 4: Overview of Mesh	12
Figure 5: Showing Three Main Spheres of Influence in Mesh.....	12
Figure 6: Mesh Refinements Near Airfoil.....	13
Figure 7: Magnified View of Mesh Refinements Near Airfoil.....	13
Figure 8: Front Edge of Airfoil	14
Figure 9: Inflation Cells in Mesh at Front Edge of Airfoil	14
Figure 10: Trailing Edge of Airfoil.....	15
Figure 11: Mesh of Area Behind Airfoil.....	15
Figure 12: Y+ of Airfoil Surface	16
Figure 13: Ansys Fluent Solution Methods	17
Figure 14: Ansys Fluent Reference Values	17
Figure 15: A. Nakayama Model A Experimental Wake Relative Velocities.....	18
Figure 16: Calculated Wake Relative Velocities.....	19
Figure 17: Comparison of SA Models - Relative Velocity of Air in 2D Space	20
Figure 18: Comparing Airfoil Surface Pressure Coefficient Between SA Models	21
Figure 19: Magnified Airfoil Surface Pressure Coefficient Plot	21
Figure 20:Airfoil Surface Skin Friction Coefficient Plot of Various Models	22
Figure 21: Magnified Airfoil Surface Skin Friction Coefficient Plot.....	22
Figure 22: Mesh Density with Velocity Measurement Locations	24
Figure 23: NASA Mesh - L3 Grid: 169x225 and 257x113, Near View	25
Figure 24: Velocity Contours with Velocity Measurement Locations	25

Nomenclature

V	<i>Velocity</i>	$\frac{\text{Meters}}{\text{Seconds}}$
a	<i>Speed of Sound in Current Conditions</i>	$\frac{\text{Meters}}{\text{Seconds}}$
M	<i>Mach Number</i>	<i>Dimensionless</i>
γ	<i>Specific Heat Ratio</i>	<i>Dimensionless</i>
C_p	<i>Specific Heat with Constant Pressure</i>	$\frac{\text{Kilojoule}}{\text{Kilogram} * {}^\circ\text{R}}$
C_v	<i>Specific Heat with Constant Volume</i>	$\frac{\text{Kilojoule}}{\text{Kilogram} * {}^\circ\text{R}}$
R	<i>Specific Gas Constant</i>	$\frac{\text{Kilojoule}}{\text{Kilogram} * {}^\circ\text{R}}$
T	<i>Absolute Temperature</i>	${}^\circ\text{R}$
R_{e_L}	<i>Reynolds Number Based on Chord Length</i>	<i>Dimensionless</i>
ρ	<i>Density</i>	$\frac{\text{Kilograms}}{\text{Meters}^3}$
c	<i>Chord length</i>	<i>Meters</i>
μ	<i>Fluid Viscosity</i>	$\frac{\text{Newtons} * \text{Seconds}}{\text{Meters}^2}$
u	<i>Velocity Parallel to Wall</i>	$\frac{\text{Meters}}{\text{Seconds}}$
u_τ	<i>Shear Velocity</i>	$\frac{\text{Meters}}{\text{Seconds}}$
y	<i>Distance from Wall</i>	$\frac{\text{Meters}}{\text{Seconds}}$
κ	<i>von Kármán Constant = 0.4187</i>	<i>Dimensionless</i>
E	<i>Constant = 0.793</i>	<i>Dimensionless</i>

Introduction

Overview of 2D Airfoil Near-Wake Case

The airfoil used for this case is a Nakayama DSMA661 airfoil, also known as a Model A airfoil, with a chord length of one meter [1] [2]. Originally, the NASA verification and validation models used 20 chord lengths to the edge of the defined farfield. Further analysis by NASA revealed that there was an impact on the coefficient of lift when the end of the flow field is defined too close to the airfoil, and a new distance of 500 chord lengths was used for NASA's updated results. However, for the model described in this report, a farfield boundary distance of 20 chord lengths is used due to element number and computational limitations. A visual representation of this case is shown below.

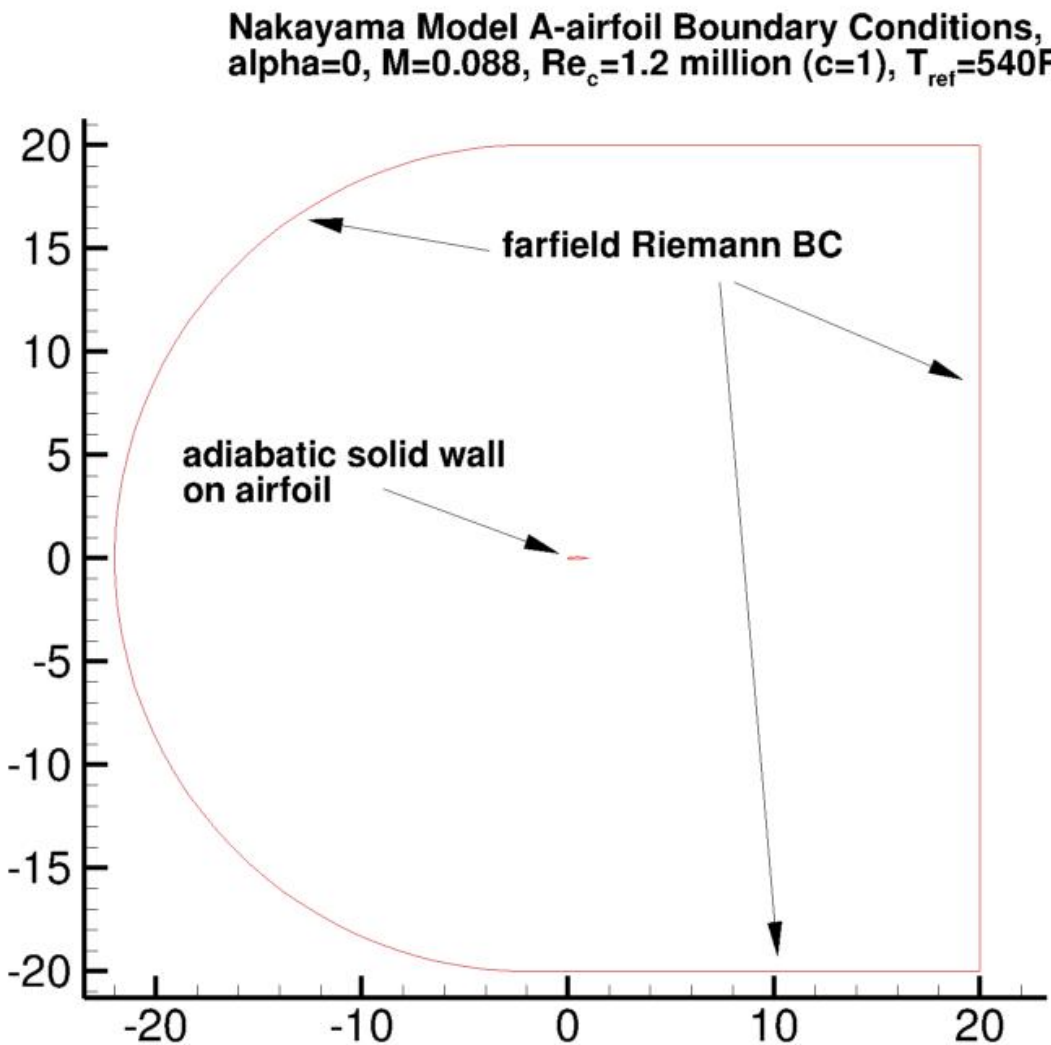


Figure 1: NASA Turbulence Modeling Resource 2D Airfoil Near-Wake Case [1] [2]

It is noteworthy that the NASA case specifies a farfield Riemann boundary condition for the farfield, and an adiabatic solid wall for the airfoil. A Riemann boundary condition is used for inflow or outflow, and depends on whether the flow at the boundary is locally supersonic or subsonic. In this case with

subsonic flow, the Riemann boundary condition prevents unwanted reflections bouncing back into the domain by providing a representation of the physical conditions at the outer boundary [3].

The airfoil is defined as having an adiabatic solid wall. This means that there is no heat transfer between the fluid and the airfoil, thus an assumption can be made that both the airfoil and fluid stream are the same temperature of 540 Rankin. In addition, the airfoil is defined as having a no-slip condition in Ansys Fluent, which means that the velocity of the fluid against the airfoil will be zero relative to the airfoil and a boundary layer will develop.

In addition to boundary layer conditions, the NASA 2D Airfoil Near-Wake (2DANW) case provides a physical description of the flow field. This case specified a fully turbulent field with an angle of attack of zero degrees, Mach number of 0.088, Reynolds number of 1.2 million, and a reference temperature of 540 Rankin [1] [2]. As mentioned on the introduction page for the 2DANW case, a Mach number of 0.088 is very low and the flow could be considered essentially incompressible. However, to ensure that the solution and resulting plots match the NASA case as closely as possible, a compressible code is used for this model. Given this information, the velocity and density of the air can be determined using the following equations.

Calculating Airspeed

The equation for the velocity of the air in this case is given by:

$$V = a * M \quad [1]$$

Where V is the air velocity in meters per second, a is the speed of sound in the air in meters per second, and M is the dimensionless Mach number. In order to find a , additional calculations must be completed as seen below.

First, the specific heat ratio of the air must be determined. Note that in some thermodynamics courses, K is used to denote the specific heat ratio instead of γ which is used here.

$$\gamma = \frac{C_p}{C_v} \quad [2]$$

In this equation γ is the dimensionless specific heat ratio of the air, C_p is the specific heat of the air with constant pressure in kilojoules per kilogram per degree Rankin, and C_v is the specific heat of air with a constant volume, similarly in kilojoules per kilogram per degree Rankin.

Once the specific heat ratio has been found, the speed of sound in the air can be calculated by using the following equation:

$$a = \sqrt{\gamma RT} \quad [3]$$

Here, R is the specific gas constant in kilojoules per kilogram per degree Rankin, and T is the temperature of the air in degrees Rankin. Using the given conditions for this case, it can be found that the velocity of the fluid stream $V = 21.7 \frac{\text{Meters}}{\text{Second}}$.

Determining Air Density

In addition to the velocity of the fluid stream, the density of the fluid (air) must be determined. Density can be found with the following equation:

$$\rho = \frac{R_{eL} * \mu}{c * V} \quad [5]$$

Where ρ is density with units kilograms per meter cubed, R_{eL} is the Reynolds number based on the chord length of the airfoil, μ is the fluid viscosity in Newton seconds per meters squared, c is the chord length of the airfoil in meters, and V is the velocity of the air in meters per second. This equation yields an air density of $\rho = 1.023 \frac{\text{Kilograms}}{\text{Meters}^3}$. Hand calculations are attached to this report as Appendix A.

Model Description

Both the CFL3D and FUN3D compressible RANS models published on the NASA site utilized the Spalart-Allmaras turbulence equation [4]. The results from these codes are the basis of comparison for the verification of this mesh and Ansys Fluent's modified Spalart-Allmaras equation. Hence, as the comparison is against Spalart-Allmaras-based cases, so too this case utilizes a variant of Spalart-Allmaras.

ANSYS Fluent's implementation of the Spalart-Allmaras equation is modified to allow for a coarser mesh to still produce useful results. The transport equation for the Spalart-Allmaras model is given by ANSYS as:

$$\frac{\partial}{\partial t}(\rho \tilde{v}) + \frac{\partial}{\partial x_i}(\rho \tilde{v} u_i) = G_v + \frac{1}{\sigma_{\tilde{v}}} \left[\frac{\partial}{\partial x_j} \left\{ (\mu + \rho \tilde{v}) \frac{\partial \tilde{v}}{\partial x_j} \right\} + C_{b2} \rho \left(\frac{\partial \tilde{v}}{\partial x_j} \right)^2 \right] - Y_v + S_{\tilde{v}} \quad [6]$$

where G_v is the production of turbulent viscosity and Y_v is the destruction of turbulent viscosity. $\sigma_{\tilde{v}}$ and C_{b2} are constants, ν is the molecular kinematic viscosity. $S_{\tilde{v}}$ is a source term defined by the user [5]. For this model, the default constants in Ansys Fluent 2023 R2 Student were used and can be seen below.

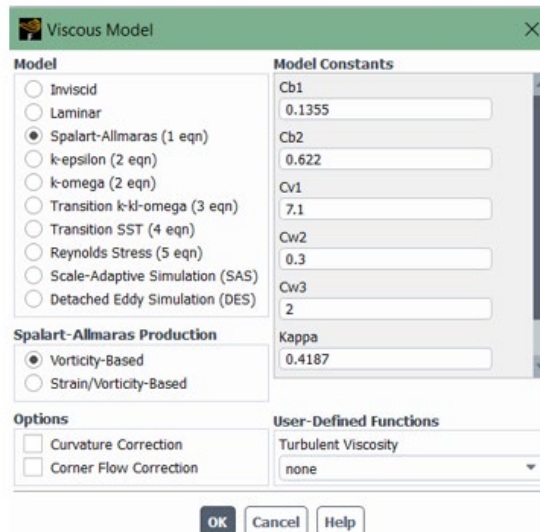


Figure 2: Ansys Fluent Viscous Model Options and SA Constants

As mentioned, there are modifications to the Spalart-Allmaras model in Ansys Fluent, which allows it to be less sensitive to numerical error when non-layered meshes are used near walls, which is useful even after implementing inflation in the meshing of the cells next to the edge of the airfoil. As published in the Ansys Fluent Theory Guide, if the mesh is sufficiently refined to capture the viscosity-dominated sublayer, the wall shear term is derived from the stress-strain relationship specific to laminar flow [6]:

$$\frac{u}{u_\tau} = \frac{\rho u_\tau y}{\mu} \quad [7]$$

Here, u is the velocity parallel to the wall in meters per second, u_τ is the shear velocity in meters per second, y is the distance from the wall in meters, κ is the von Kármán constant (0.4187), and $E = 9.793$.

However, if the mesh is not sufficiently refined, then it is presumed that the central point of the cell adjacent to the wall lies within the logarithmic region of the boundary layer, and the law-of-the-wall is applied as shown in equation [8].

$$\frac{u}{u_\tau} = \frac{1}{\kappa} \ln E \left(\frac{\rho u_\tau y}{\mu} \right) \quad [8]$$

In this equation κ is the von Kármán constant = 0.4187, and the dimensionless distance $E = 9.793$ [6]. In the realm of fluid dynamics the law of the wall, also referred to as the logarithmic law of the wall, asserts that the average velocity within a turbulent flow at a specific location correlates with the logarithm of the distance from that point to the "wall" or the fluid region's boundary.

Remainder of Page Intentionally Left Blank

Mesh

Mesh methodology

The geometric point-definition of the airfoil shape that this model is based on is given on the 2DANW introduction page as the “DSMA661 as-created point definition” [1]. The original points provided in that file defined a non-smooth curve, however the other grid definition published on the NASA website defined a blunt trailing edge which did not match the airfoil used in the NASA solutions. In order to smooth the trailing edge of the airfoil, avoid overlapping geometry, and close the trailing edge, every fifth data point of the sharp-edge point-definition was taken to create a new, smoother profile. While this does not capture the exact airfoil geometry used by NASA models, it does define a smoother representation of the airfoil and avoids issues with overlapping geometry that was included in the original definition. The modified airfoil grid definition used for the model in this report is attached as Appendix B.

The methodology for developing and refining the mesh for this model was relatively straightforward. The goal was to capture the behavior of the fluid stream along the airfoil, as the wake is heavily dependent on airfoil geometry. The value used to determine whether grid independence had been reached was $Y+$ at the middle ($x/c = .5$) of the airfoil’s top surface.

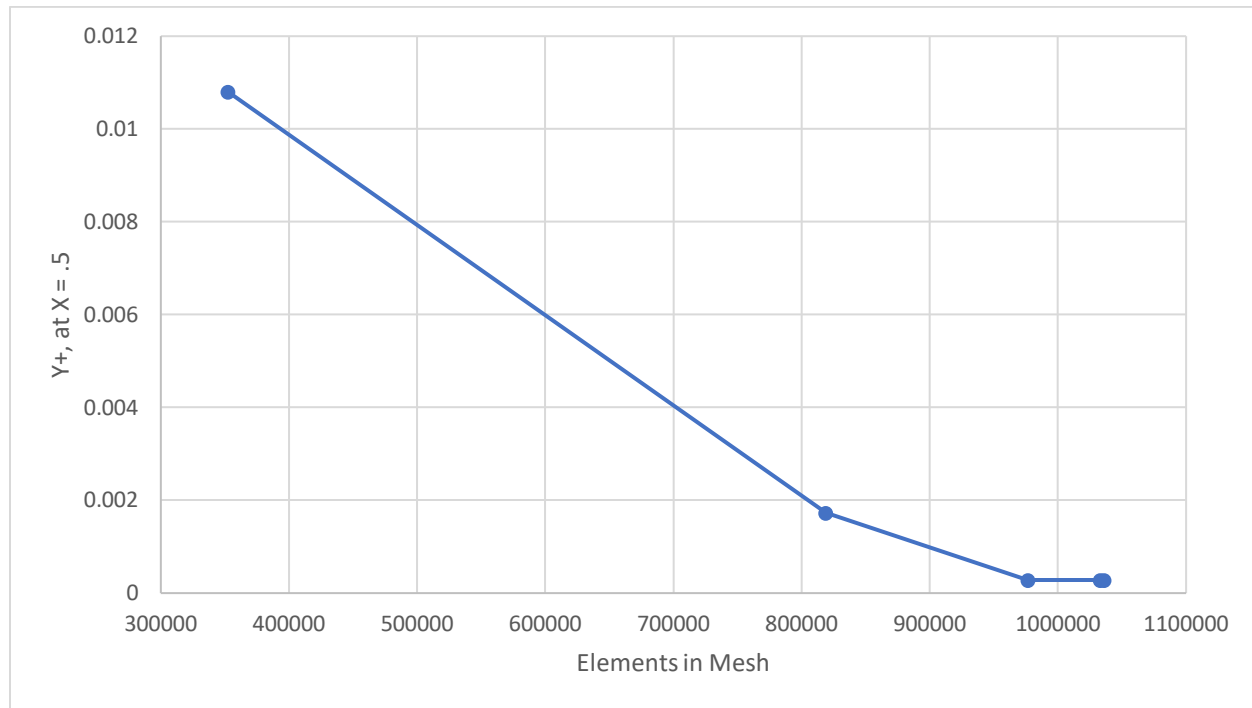


Figure 3: Convergence Criteria of $Y+$ and Number of Elements

Due to the definition of the mesh geometry, there was a large jump in the number of elements defining the background between the first and second refinements from 352492 to 818929 elements, as there were convergence issues when increasing the density of the mesh only near the airfoil surface. As pictured in Figure 2, it appears that that grid independence has been reached using $Y+$ of the airfoil as a method of comparison.

Mesh Description

The final mesh for this model is comprised of 1035848 elements, just a few thousand under the 1048576 limit for the student version of Ansys Fluent. With this many elements it is difficult to make out individual cells at this zoom level.

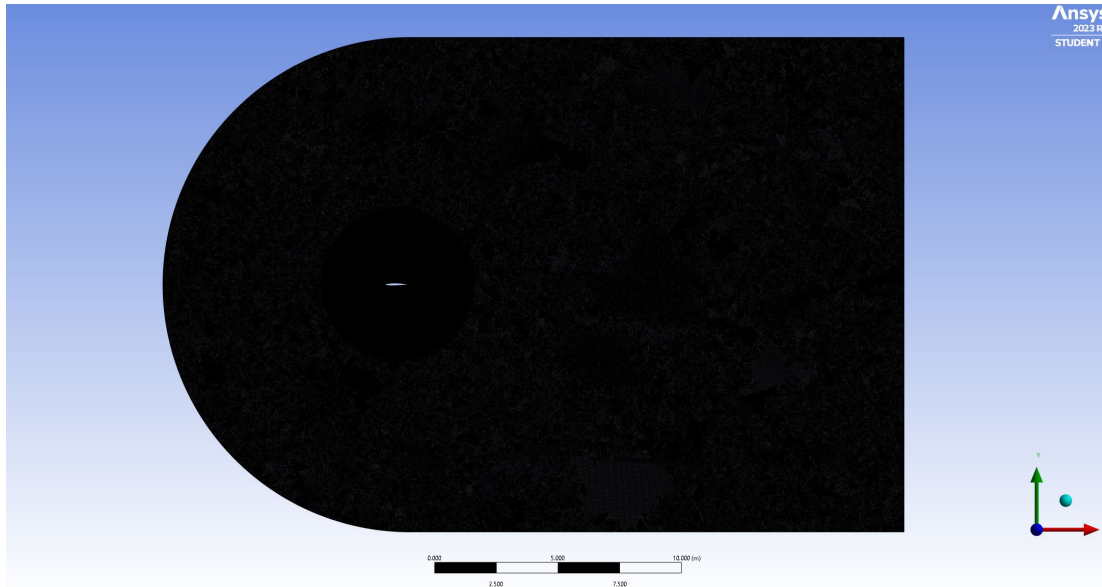


Figure 4: Overview of Mesh

A better representation of mesh density between spheres of influence can be seen below. This mesh has background elements with individual sizes of $.04 \text{ m}^2$, the largest sphere of influence is 3 meters in diameter with elements of area $.025 \text{ m}^2$, and the smaller sphere of influence is 0.75 meters in diameter with an element size of $.075 \text{ m}^2$.

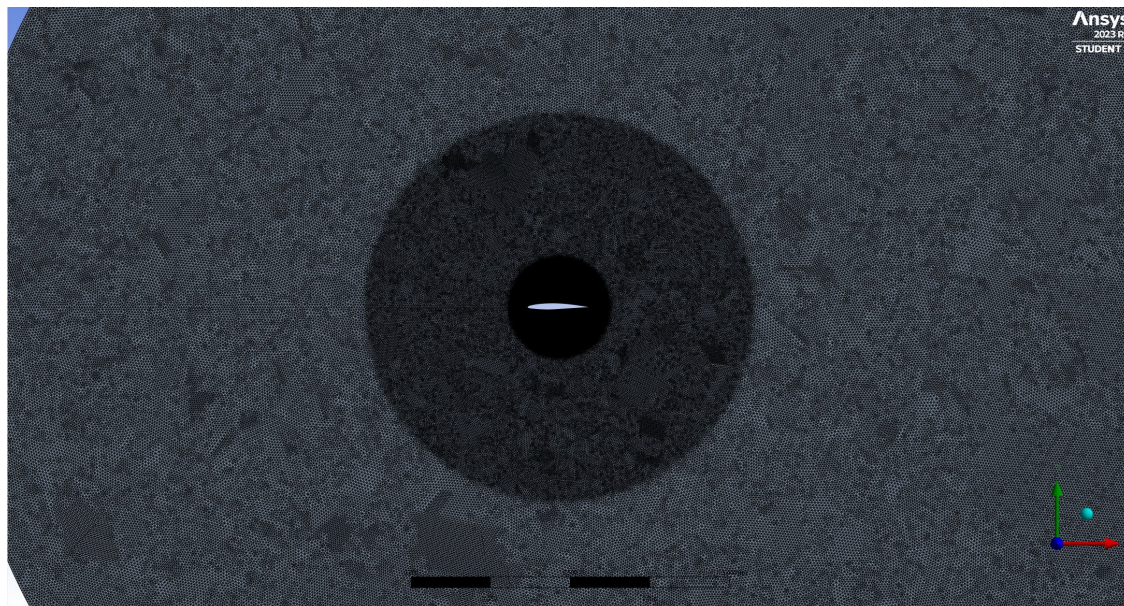


Figure 5: Showing Three Main Spheres of Influence in Mesh

Figure 5 shows the mesh in further detail, and the inclusion of four evenly spaced 0.2-meter diameter spheres of influence with elements of size 0.005 m^2 . This geometry was determined by trial and error, as size and placement of these spheres of influence had a large impact on the total element count and the convergence.

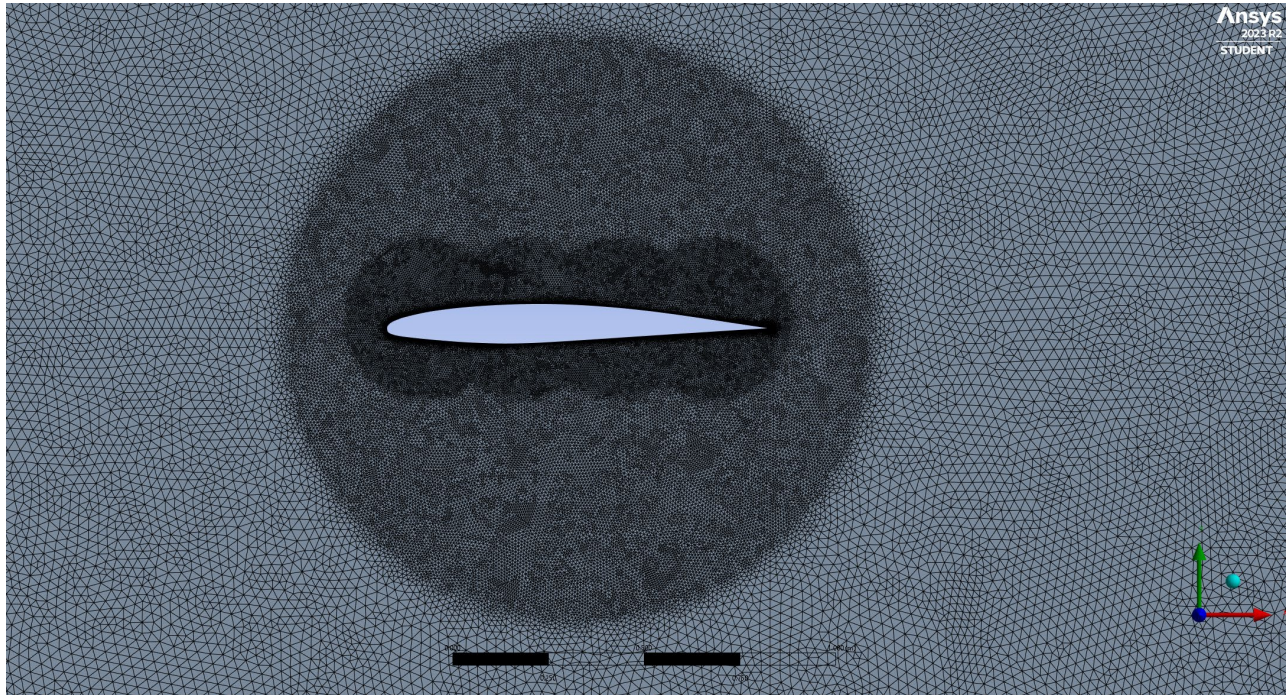


Figure 6: Mesh Refinements Near Airfoil

In Figure 6, the very fine mesh around the airfoil can be seen. The top and bottom edges of the airfoil each had 1500 elements along each side for a total of 3000 elements defining the airfoil profile. This was necessary to capture the behavior of the air near the surface of the airfoil.

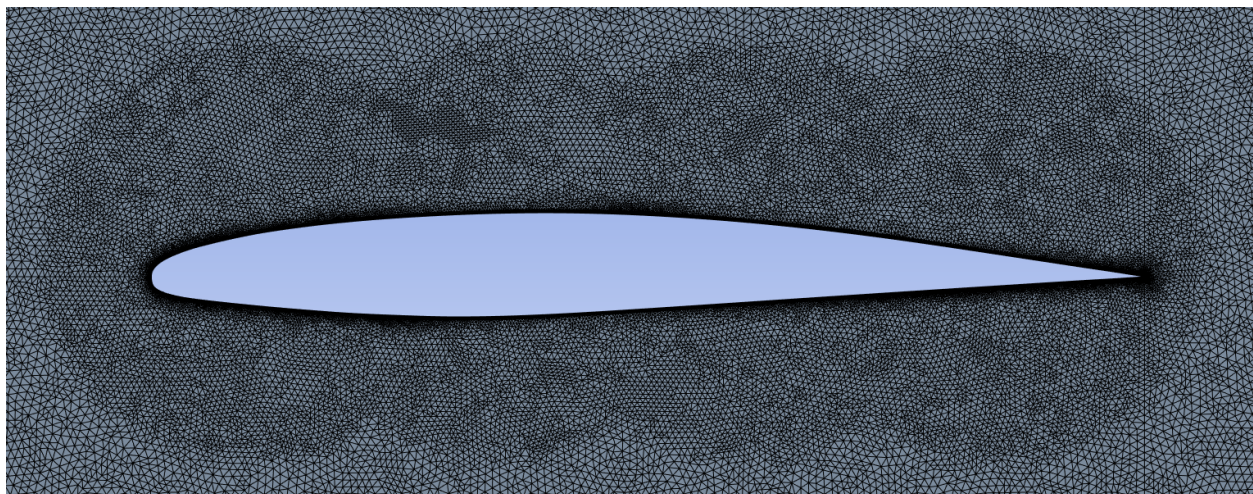


Figure 7: Magnified View of Mesh Refinements Near Airfoil

While elements along the airfoil edge are important for determining the behavior of the air with regards to the airfoil surface, the inflation method pictured in Figure 7 and Figure 8 play a large role in ensuring

the viscous effects of the boundary layer are captured. The inflation method used was defined to have 50 total layers at a total thickness of .0025 meters, with the growth rate being determined by those parameters.

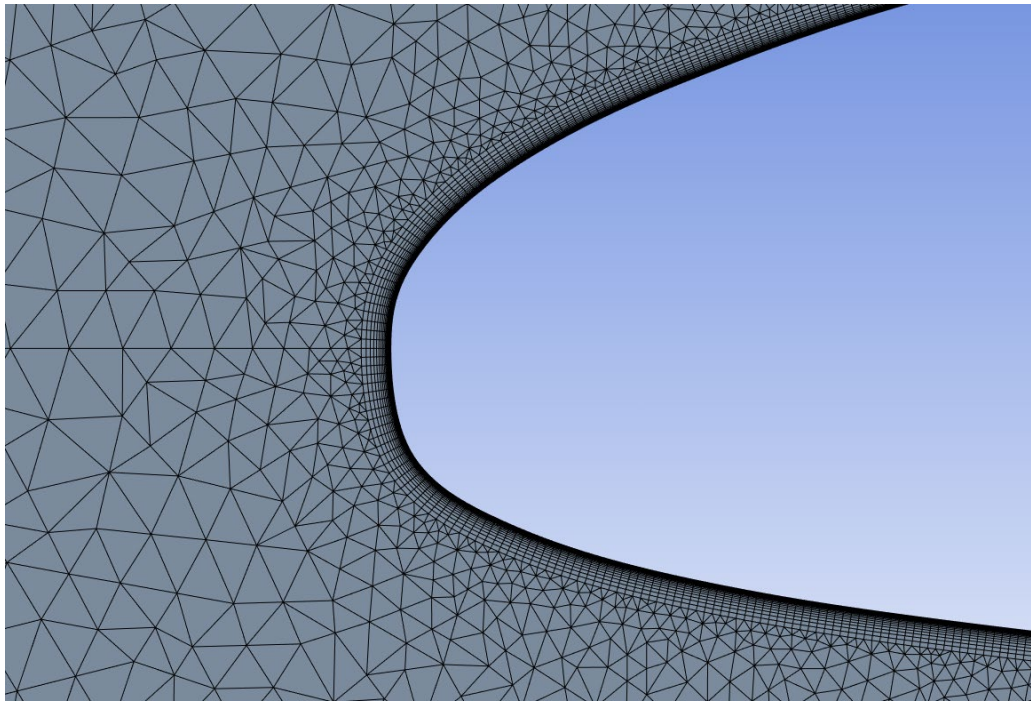


Figure 8: Front Edge of Airfoil

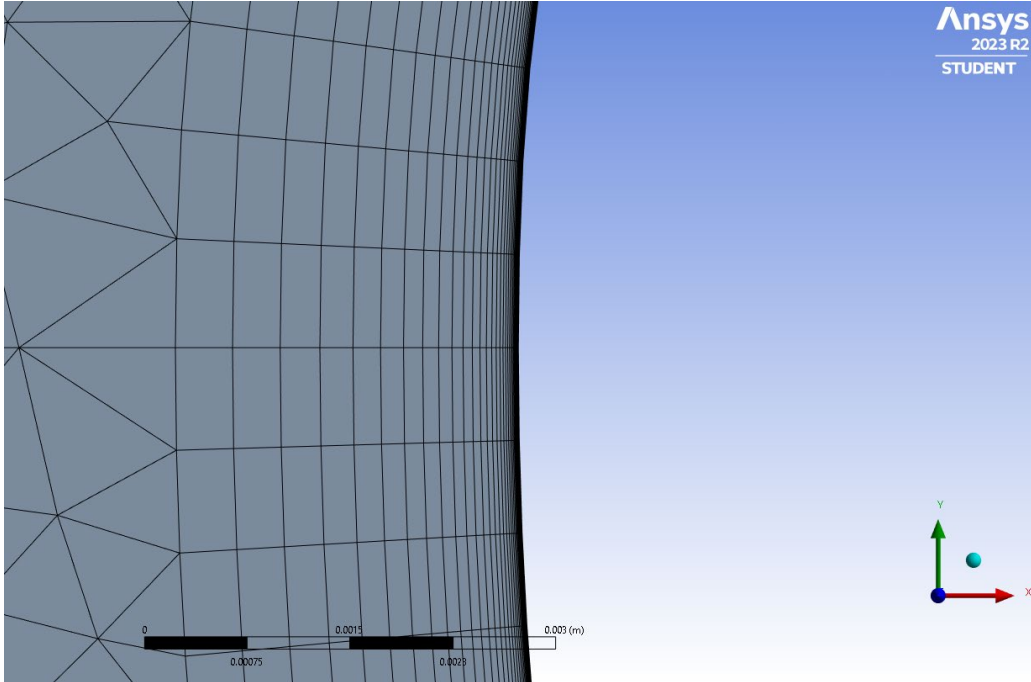


Figure 9: Inflation Cells in Mesh at Front Edge of Airfoil

The trailing edge of the airfoil can be seen in Figure 9 below. Note the density of the mesh with regard for the airfoil.

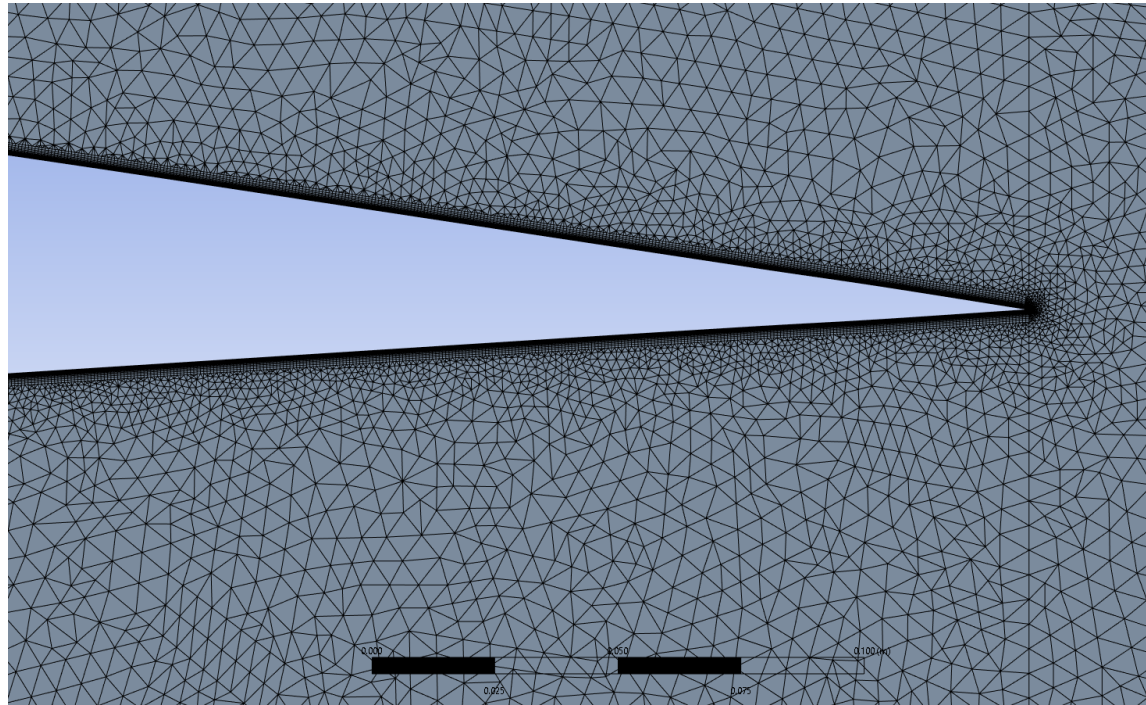


Figure 10: Trailing Edge of Airfoil

Figure 10 shows the area of the mesh behind the airfoil, where the wake will be measured after a solution is calculated. The focus when meshing was to capture the behavior of the air near the airfoil. However, the case this report is comparing against requires analysis of the behavior of the air in the wake of the airfoil. Notably there are no areas of influence to refine the mesh in the region of interest.

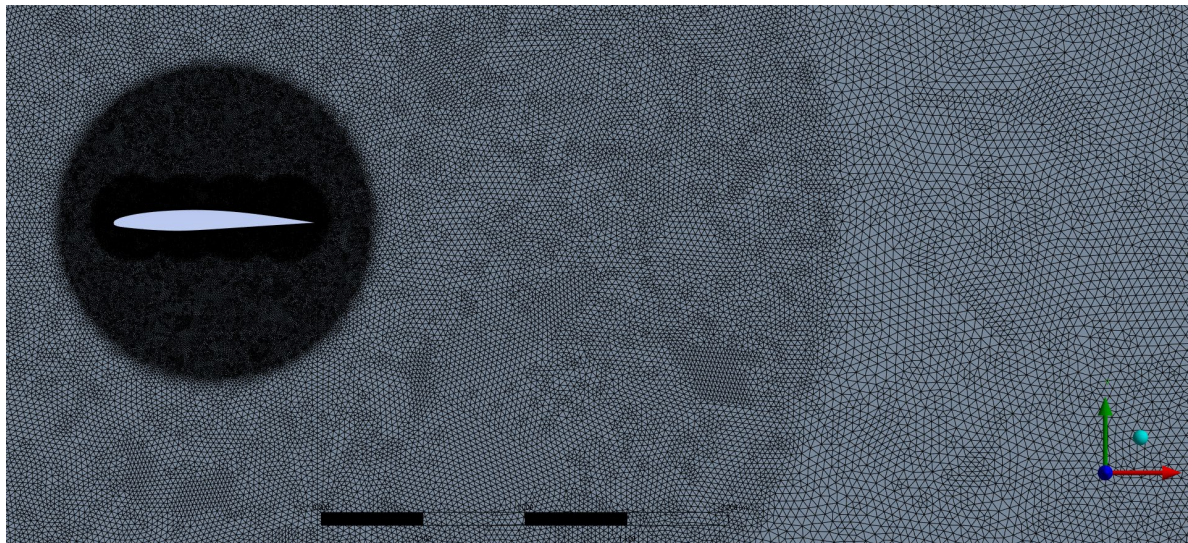


Figure 11: Mesh of Area Behind Airfoil

Airfoil Surface $Y+$

As mentioned in the model description, Ansys Fluent utilizes a Spalart-Allmaras equation that has been modified to produce usable results even when the mesh near a surface is not refined as much as is needed for the original equation to be used [6]. Thus, the primary focus when refining the mesh was to measure grid independence by examining $Y+$ of the airfoil surface. As can be seen in the mesh description section above, the elements are smaller near the airfoil. To capture the viscous effects within the boundary layer, inflation methods were used at the edge of the airfoil, as it is well-known that the gradients differ more significantly in the normal direction relative to the surface. A dimensionless number, $Y+$, describes how fine or course a mesh is near the surface. The $Y+$ value for the airfoil surface in this solution is shown below:

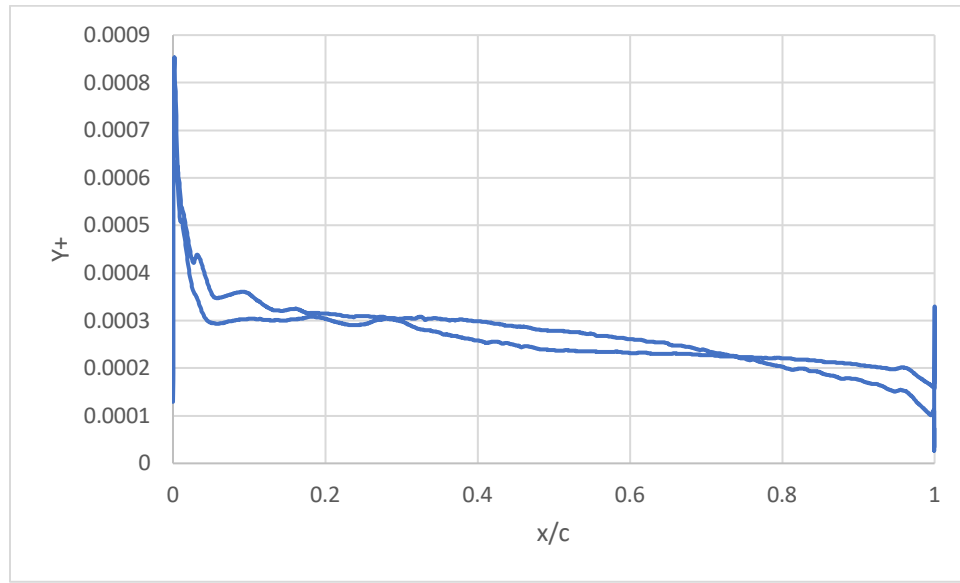


Figure 12: $Y+$ of Airfoil Surface

As can be seen in the figure above, Ansys Fluent calculates the $Y+$ value for the entire mesh along the airfoil to be orders of magnitude under one. Generally, a low $Y+$ value would be a good sign, as this indicates that the first grid cell is located within the laminar sublayer. However, an extremely low value like this could lead to a lack of accuracy of turbulent behavior near the boundary layer [7].

Solution Methods

Before the solution can be calculated using the mesh described in the previous section, Ansys Fluent requires initialization of each cell. That is, initial values must be determined as a starting point so that the solver can start the simulation. For this model the hybrid initialization option was used as it often outperforms the standard method in terms of providing a more accurate starting point. This is useful as a more accurate initial guess results in a decreased time to reach convergence, and increased simulation stability. In order to determine when the solution has converged, residual monitors were used. For this model the residual monitor thresholds were set to 1E-06 to balance solution precision and computation time.

The solution methods for this model were kept to the default values as there were no issues with convergence using the refined mesh. The solution methods task page is shown in Figure 12.

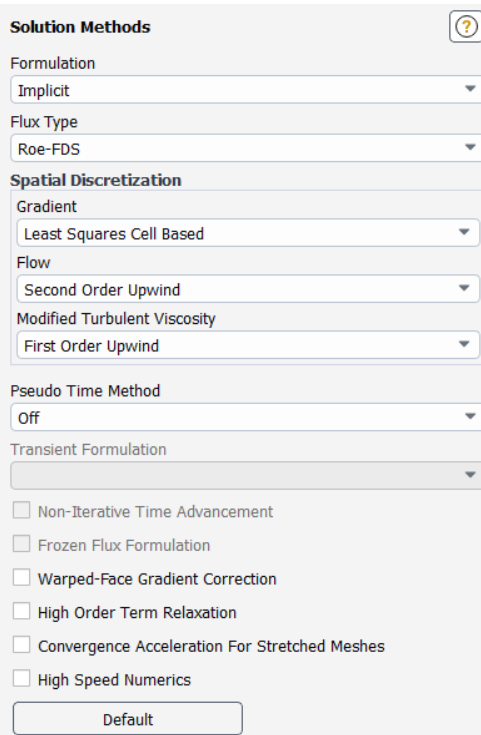


Figure 13: Ansys Fluent Solution Methods

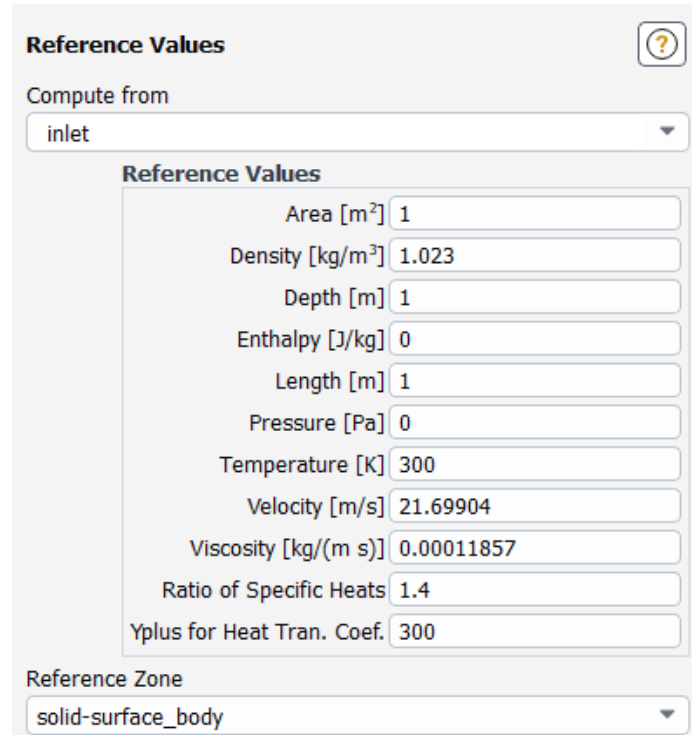


Figure 14: Ansys Fluent Reference Values

While the solution methods were kept to their default settings, the reference values used for this solution were based on the properties of the fluid at the inlet. The derivation and calculation of these values are discussed in the introduction to this case, however for ease of reading, the reference value task page from Ansys Fluent is shown in Figure 13.

Verification

As mentioned previously, this model will be verified by comparing results from CFL3D and FUN3D compressible code published on the NASA Turbulence Resource website. The published results provide data that describes the relative velocity of the fluid at varying distances from the trailing edge of the airfoil, that is, the near wake behavior of the fluid. The Spalart-Allmaras-based CFL3D and FUN3D results are shown below alongside the results from this report. Note that no data from $x = 1.01$ was gathered for this case possibly due to nodal points not aligning with the line generated in Ansys Fluent to create an x-y plot. Due to difficulties generating datapoints for the $x = 1.01$ and $x = 3$ meters the comparison will only include four x locations: 1.05, 1.2, 1.4, and 1.8 meters from the trailing edge. Note that the airfoil is one meter long, so the relative y/c position is already normalized and equal to that same y-position in space.

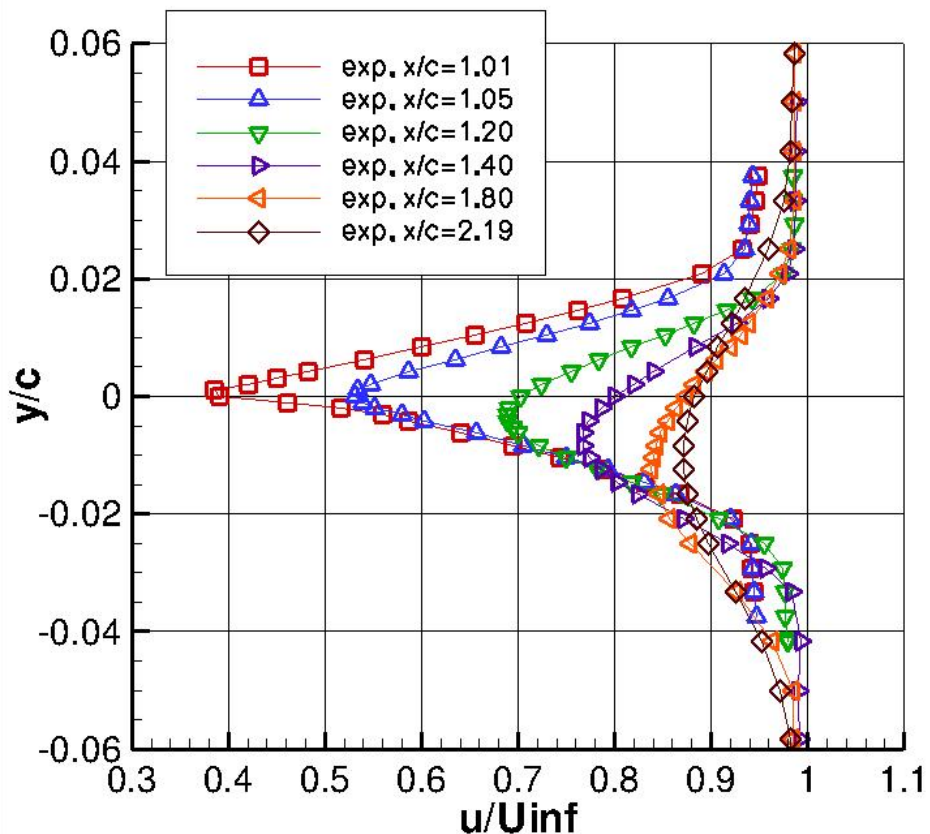


Figure 15: A. Nakayama Model A Experimental Wake Relative Velocities

The study that this data was pulled from, "Characteristics of the Flow around Conventional and Supercritical Airfoils," by Nakayama, A. was behind a paywall [2]. Thus a comparison between two different plots must be made between the experimental data and the results of the simulation defined by this report, though admittedly this method of comparison is less than ideal.

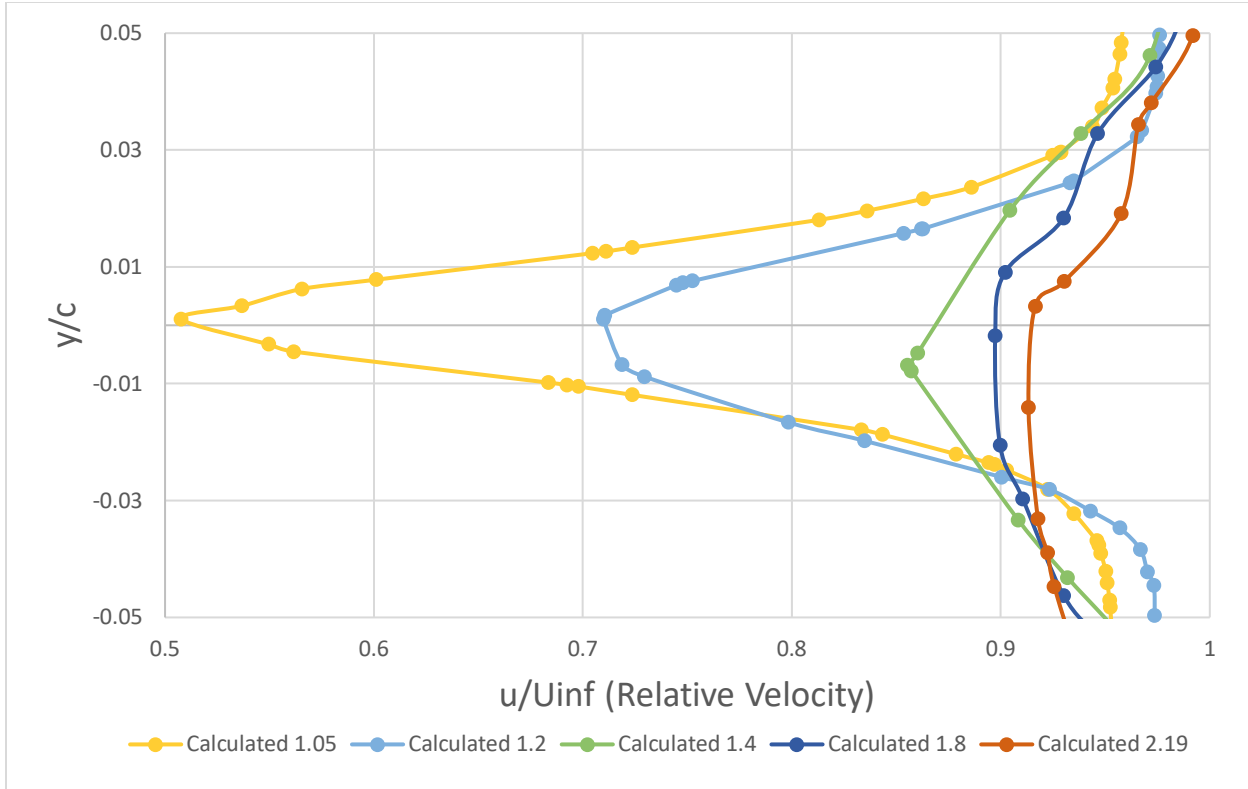


Figure 16: Calculated Wake Relative Velocities

There are a few notable differences between the experimental results and the calculated results, shown in Figure 14 and Figure 15 respectively. The calculated results follow the general trends experimental results, with slightly offset relative velocities. However, while the behavior of the fluid near the airfoil was captured well and agrees with NASA's solution as detailed earlier, the mesh was not refined enough in the wake trailing the airfoil to provide useful results. The $x = 1.2$ and $x = 1.4$ lines had 17 and 18 data points defining the curve in the graph respectively, which highlights not only the need for a finer mesh in that area, but provides a reason for the non-smooth and uneven behavior in Figure 2, and these points were not evenly distributed which exacerbated the problem. Regardless, the comparison does show general agreement, though not as precisely matching as expected.

Validation

While verification compares against experimental results, validation seeks to evaluate against experimental results. Figure 16 below shows the same calculated results from the model outlined in this report as the dotted lines, plotted against the CFL3D and FUN3D SA models.

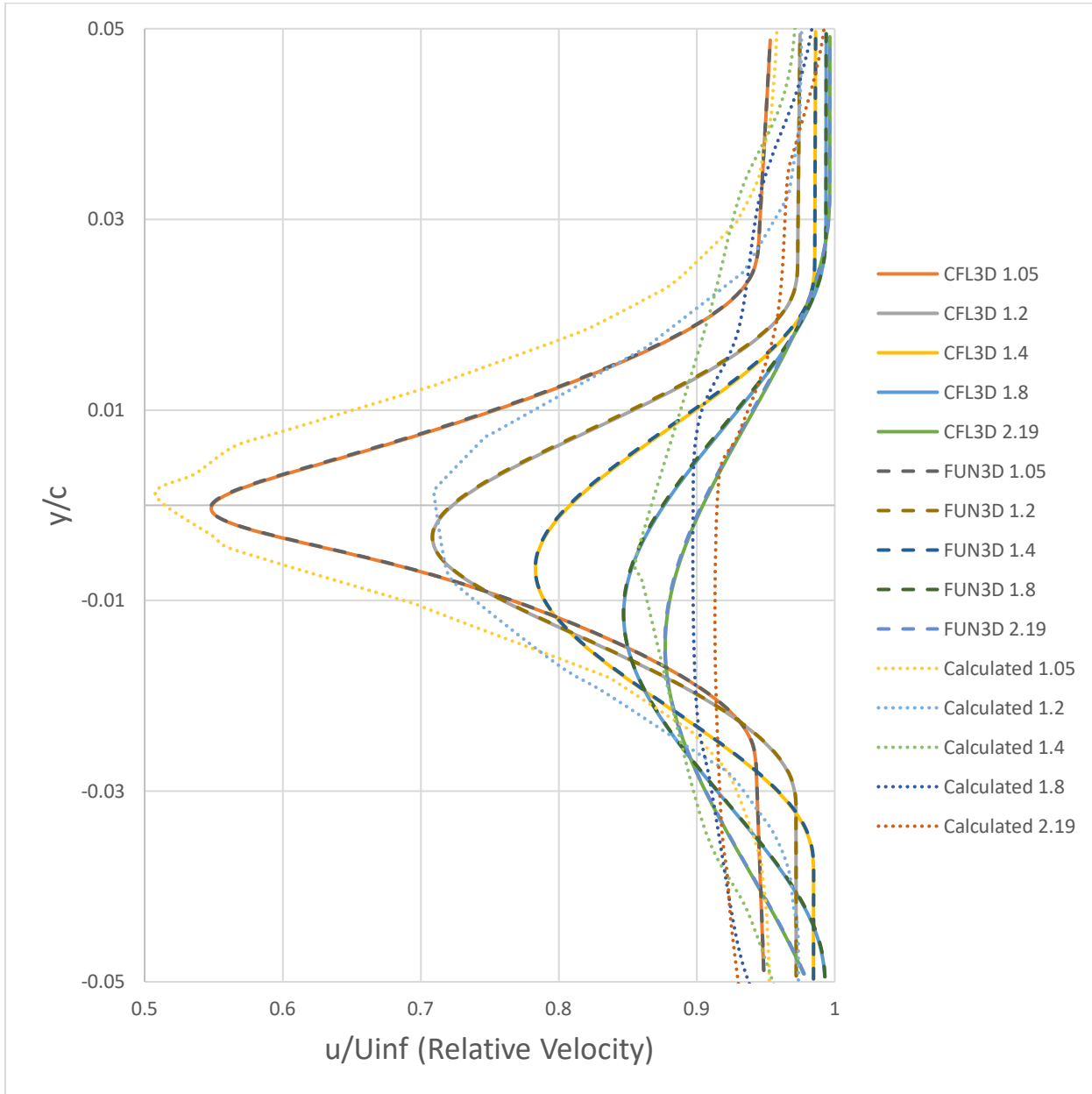


Figure 17: Comparison of SA Models - Relative Velocity of Air in 2D Space

The calculated results as shown follow the general trends of the NASA CFL3D and FUN3D solutions. As in the verification comparison, the calculated relative velocities shown here are slightly off compared to both NASA CFD solutions. Note again that the captured behavior of the fluid closer to the airfoil, such as $x = 1.05$ and $x = 1.2$ meters is more closely matching the NASA models than the locations more distant from the airfoil.

Besides relative velocity, the NASA validation case provides two additional graphs to compare against; Airfoil pressure coefficient and skin drag friction are both plotted against x/c where the chord length of the airfoil is equal to one.

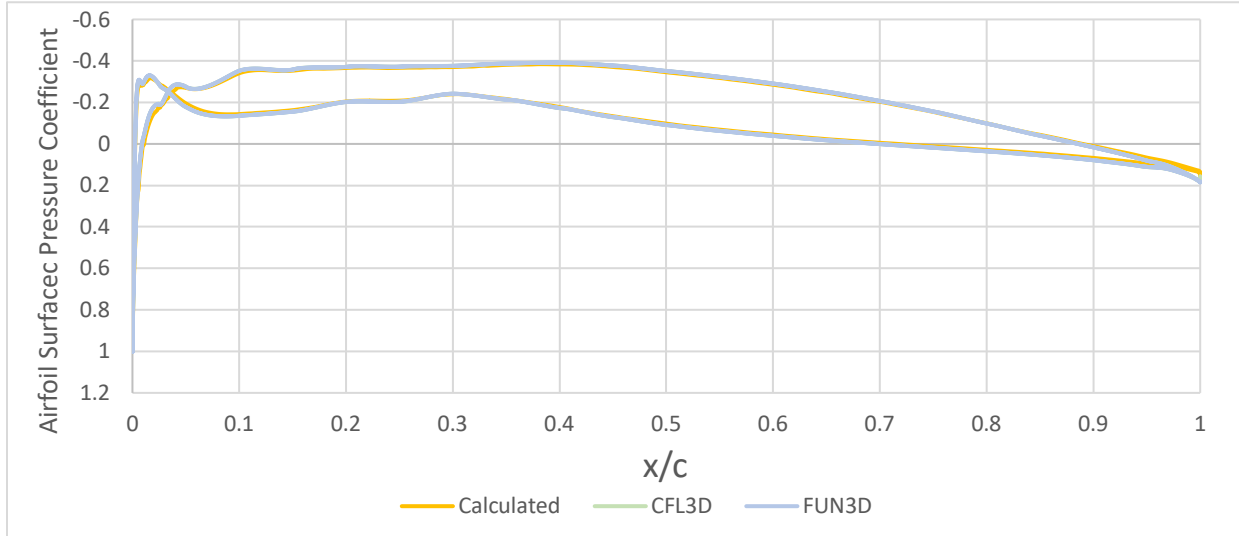


Figure 18: Comparing Airfoil Surface Pressure Coefficient Between SA Models

As seen in Figure 3, the airfoil surface pressure coefficient calculated by this model correlates very well with both the CFL3D and FUN3D NASA models. To explore this further, a more detailed view is shown by Figure 4, where the vertical axis has been changed to focus on the majority of the plotted data.

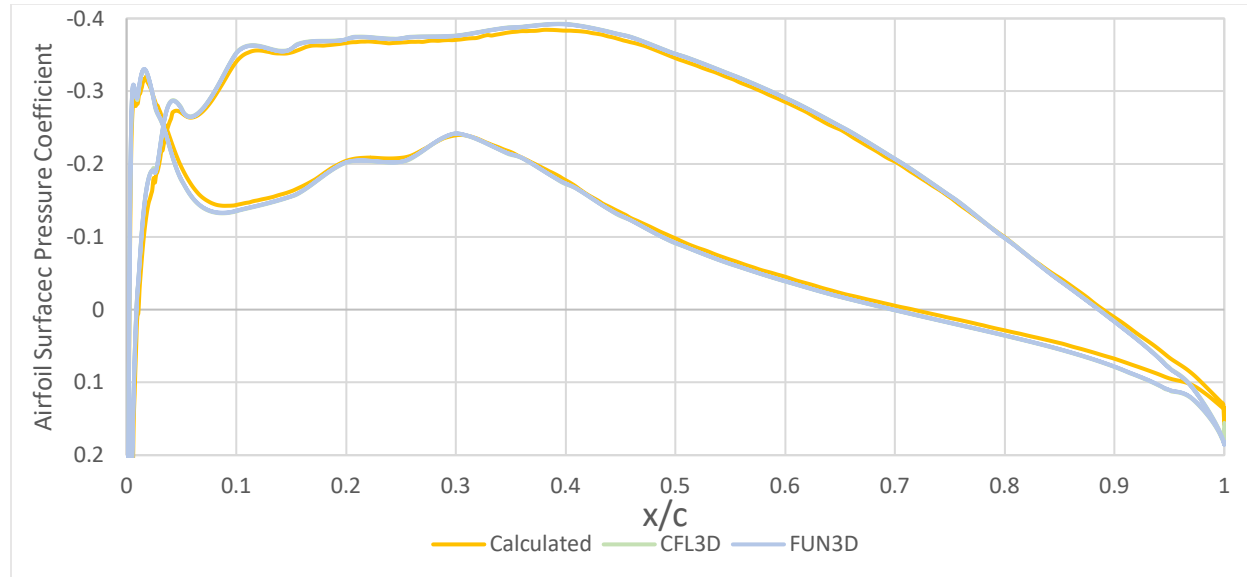


Figure 19: Magnified Airfoil Surface Pressure Coefficient Plot

Admittedly, the results from the NASA models are almost indistinguishable from one another on the plot whereas the results from the model outlined in this report are slightly offset in many areas. One noteworthy area is the trailing edge of the airfoil, where the models are the most different. However in general, all three models describing the behavior of air near the airfoil surface produce similar results.

Another comparison between the CFL3D and FUN3D models, as well as the model outlined in this report, can be made via the skin friction coefficient of the airfoil surface. Note that the skin friction coefficient determined by the report model correlates with the Y+ graph shown earlier in Figure 11.

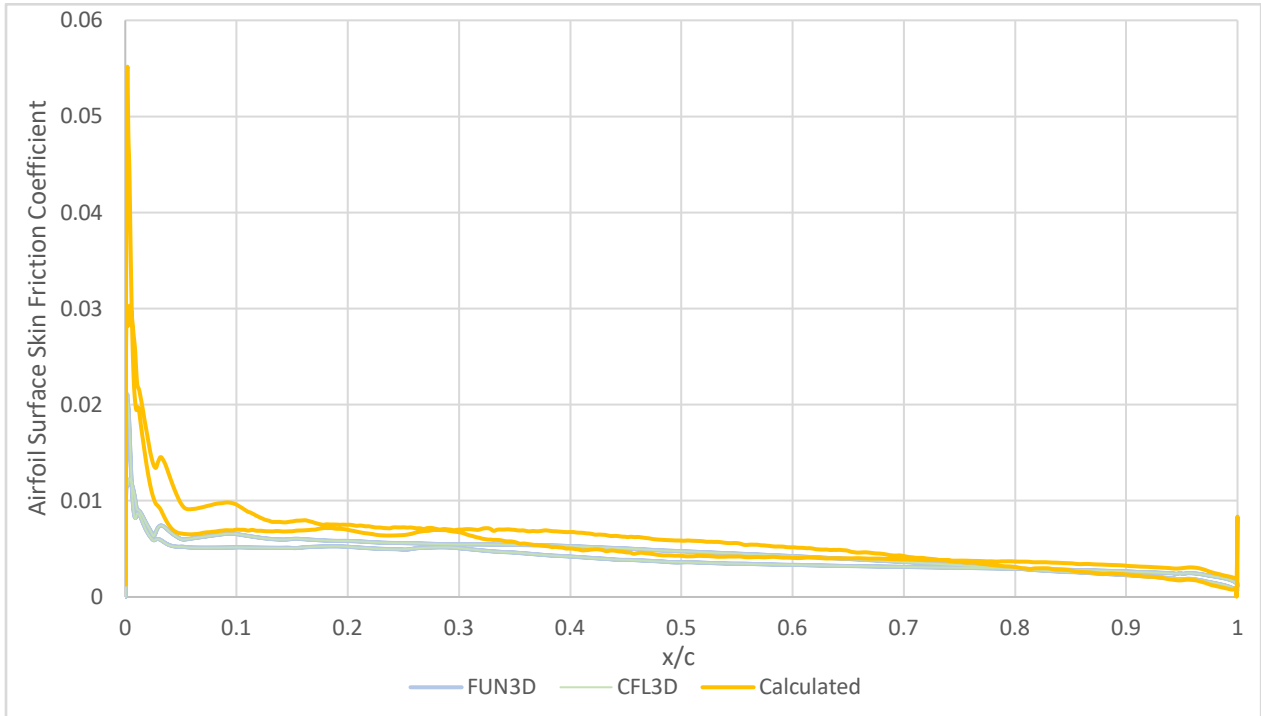


Figure 20: Airfoil Surface Skin Friction Coefficient Plot of Various Models

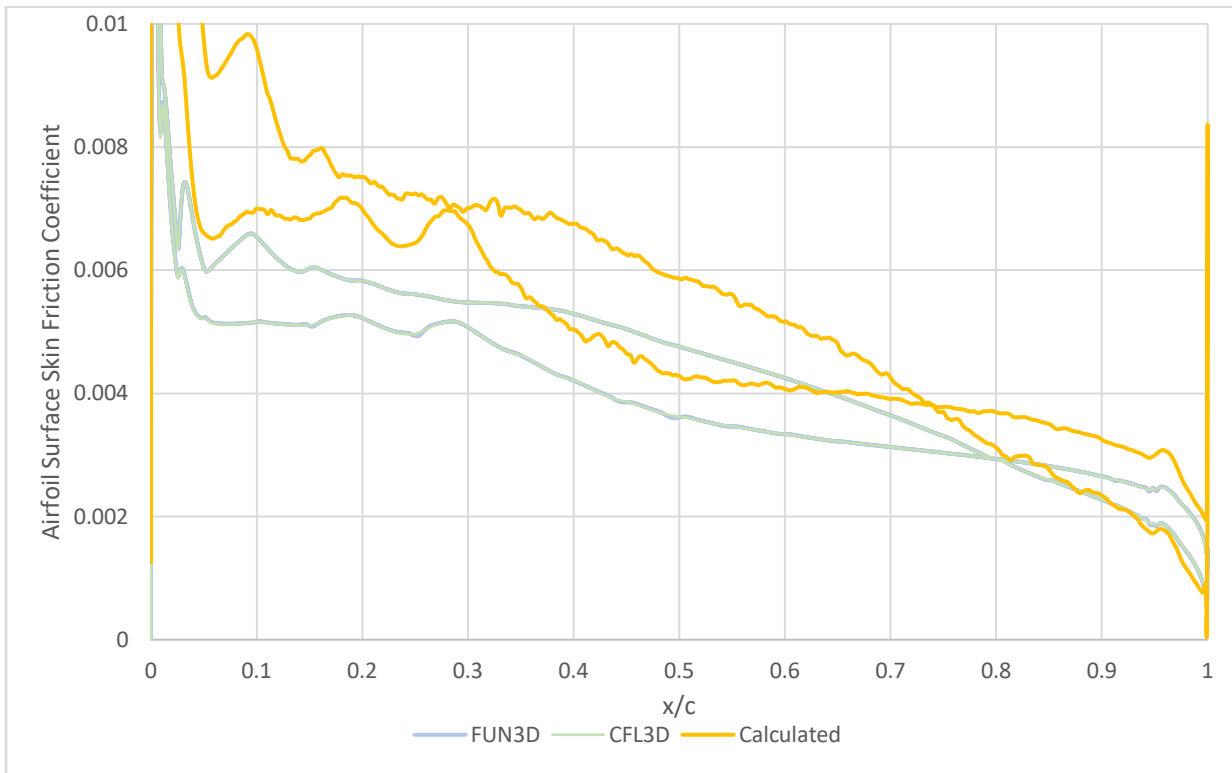


Figure 21: Magnified Airfoil Surface Skin Friction Coefficient Plot

As seen in Figure 20, the airfoil surface skin friction coefficient of the report model follows the same trends as the FUN3D and CFL3D models. However, it is offset significantly in some locations. Between $x/c = 0$ and $x/c = 0.35$, both the top and bottom airfoil surface skin friction coefficients of the report model are larger than the comparable surfaces of the FUN3D and CFL3D models. There are more significant deviations at the extreme values of $x/c = 0$ and $x/c = 1$, at the airfoil leading and trailing edges.

Remainder of Page Intentionally Left Blank

Results and Discussion

Results Overview

Overall, the model developed and defined within this report captured the behavior of the fluid interacting with the airfoil well. As shown in Figure 6, Figure 7, Figure 8, and Figure 9, the airfoil surface coefficients of pressure and skin friction coefficients generally align with what was produced by NASA's CFL3D and FUN3D models. Unfortunately, the results of this model for the wake near the trailing edge of the airfoil were lackluster in comparison to the performance of the model near the airfoil surface. This seems to be an issue caused by mesh density in the airfoil wake.

Issues with Meshing Approach

Because of the focus on refining the airfoil edge in an effort to capture the result of the airfoil moving through the flow-field, there was not an appropriately sized grid describing the wake of the airfoil. This resulted in issues when attempting to capture the behavior of the air in the wake, particularly at distances greater than $x = 1.5$. An illustration of this can be seen below. A version of this image with velocity contours instead of the mesh can be seen in Figure 24.

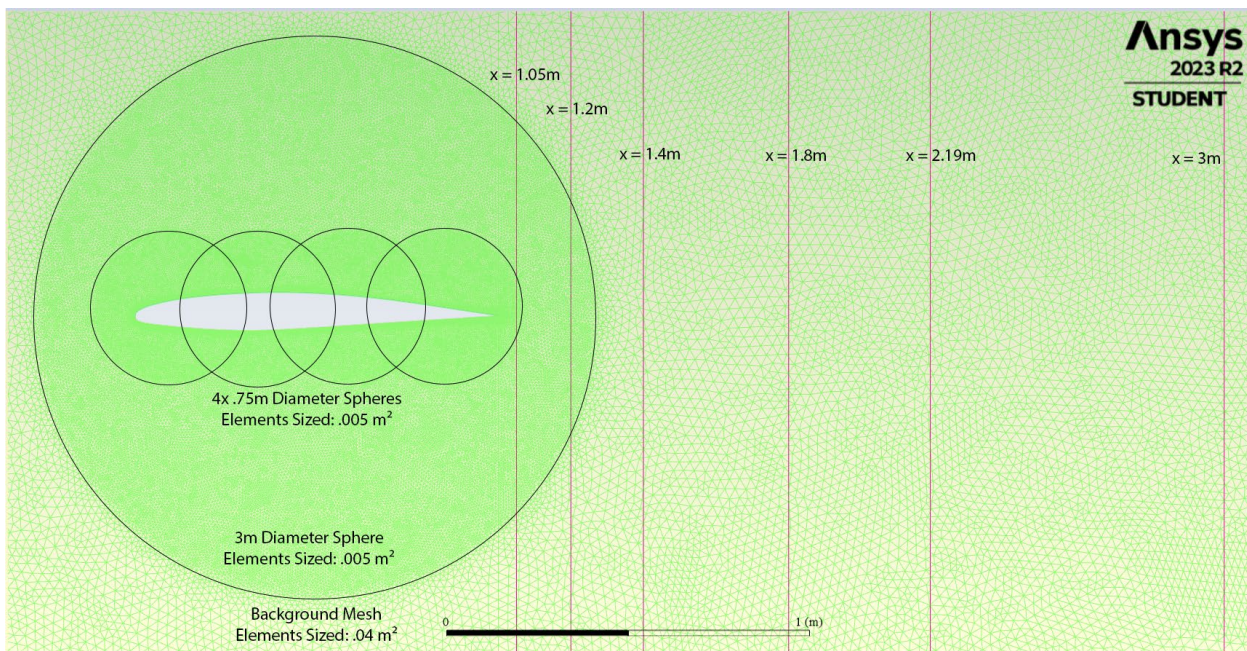


Figure 22: Mesh Density with Velocity Measurement Locations

As shown above, the density of the mesh in the wake was much less compared to the density directly surrounding the airfoil surface. However, due to element constraints a mesh could not be developed that would maintain grid independence around the airfoil while significantly increasing the density of the mesh in the airfoil wake. As mentioned previously the student version of Ansys Fluent has a 1048576-element limitation, and this mesh with a coarse wake was made up of 1035848 elements. Still, the lack of mesh refinement in the wake is a significant error that heavily impacted the measurements of the model and therefore the results of this report.

The mesh that NASA used for the CFL3D and FUN3D models included more elements in the wake, and was less dense in the area surrounding the airfoil. The mesh used for this report can be seen in Figure 10 and the NASA mesh can be found on the next page as Figure 10.

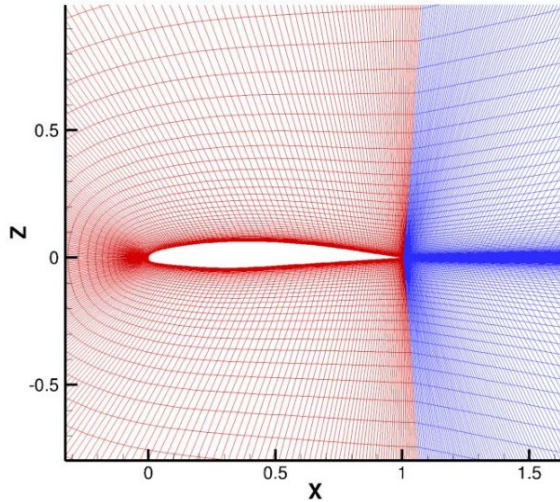


Figure 23: NASA Mesh - L3 Grid: 169x225 and 257x113, Near View

Additional Results

While the quantitative results of the wake did not match exactly with what was expected, the model does behave intuitively. Shown in Figure 23 is a velocity contour graphic with meshing and velocity measurements overlaid. The velocity profile of the wake does behave as expected. However, to generate this graphic Ansys Fluent simply interpolates between the points displayed in Figure 15, and while this data produces a graphic that looks correct, it contains the same issues already detailed in this report.

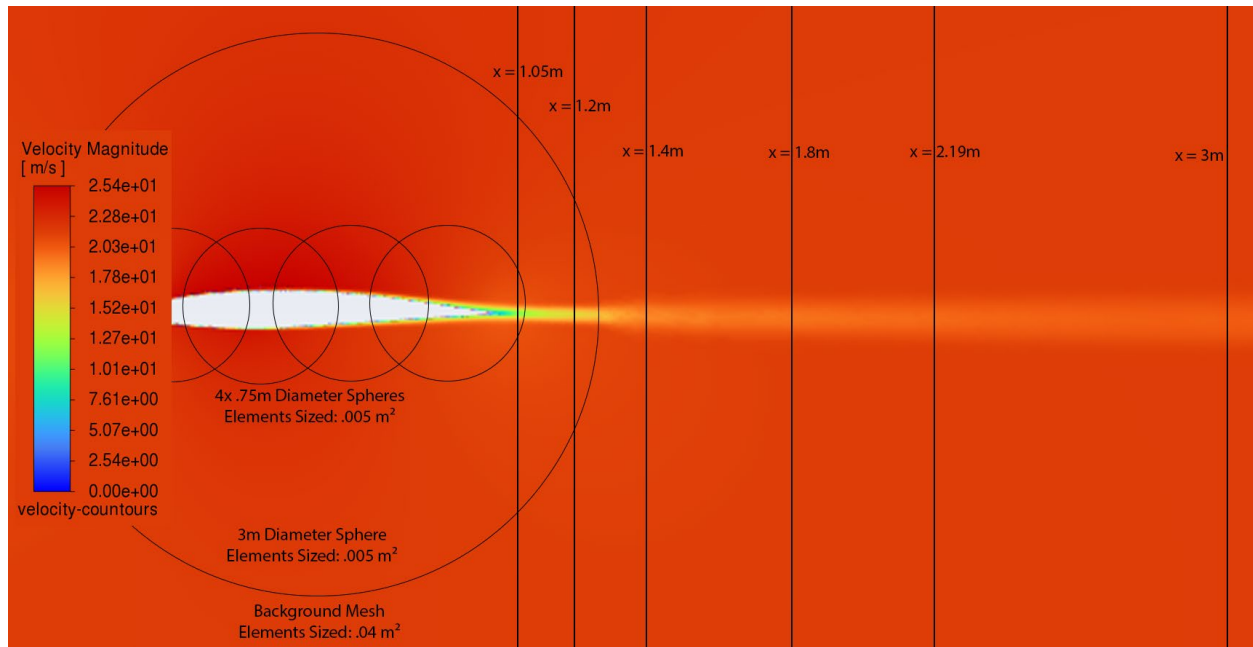


Figure 24: Velocity Contours with Velocity Measurement Locations

Another interesting finding was that the airfoil coefficient of lift found by this model did not approach the same value that NASA's CFL3D and FUN3D models did. The model developed for this report produced a coefficient of lift of .14941 and was decreasing with additional refinement, away from the NASA models which both were trending towards .16. As mentioned earlier it may have been possible that the $Y+$ value was too low and not properly capturing the behavior of the viscous layer. In future CFD applications it is advisable to determine an ideal $Y+$ range prior to meshing, and only refine the mesh near a surface until its $Y+$ value is in that range.

A significant limitation in the development of the mesh was the limitation to 1048576 elements and only four parallel processes. When the process limitations were combined with the already somewhat limited processing capability of an average desktop computer, any changes to the mesh or solution parameters would take nearly four hours to converge, thus time was another factor in the iterative process mesh refinement. It is a lengthy process to create a new meshing scheme and refine it rather than continuing to refine the current mesh, which contributed to the continued use of the flawed meshing method. While relatively user friendly, using Ansys Fluent to validate and verify a custom mesh for this 2DANW case resulted in a more time-consuming project due to the artificial bottlenecks resulting in long simulation times. For any further development and analysis of this case, it is recommended that OpenFOAM is used to avoid both the element and processor limits.

Conclusions

This project has offered valuable insights into the intricacies of computational fluid dynamics (CFD) and the nuanced process of developing a CFD mesh and solution. Despite certain flaws in the methodology, especially in addressing wake characteristics with regards to areas of mesh refinement, the model developed in this report captured the behavior of the air near the airfoil comparably to NASA's CFL3D and FUN3D models. Mesh and solution development, constrained by 1048576 elements and only four parallel processes, resulted in a solution that exhibited a strong correlation with NASA's CFL3D and FUN3D models near the airfoil though it yielded poor results further along the wake.

Interestingly, while it closely resembled results from NASA's CFD models near the airfoil, the project model exhibited notable discrepancies, particularly at the trailing edge, emphasizing the need for the mesh to be reevaluated. The solution presented in this report generally aligns with NASA's Spalart-Allmaras model for this case and the confirmation of grid independence near the airfoil through the use of $Y+$ values adds a layer of credibility to the results. However, it is acknowledged that the calculated coefficient of lift at the finest mesh did not precisely match the reported values from NASA's FUN3D and CFL3D calculations. Nonetheless, a positive aspect is the observed agreement between the coefficient of pressure and skin drag friction values across the airfoil, providing a foundation for future refinement and optimization of the meshing strategy.

References

- [1] Christopher Rumsey, NASA Langley Research Center, "VERIF/2DANW: 2D Airfoil Near-Wake Verification Case - Intro Page," November 2011. [Online]. Available: <https://turbmodels.larc.nasa.gov/airfoilwakeverif500c.html>.
- [2] A. Nakayama, "Characteristics of the Flow around Conventional and Supercritical Airfoils," *J. Fluid Mech.*, vol. 160, pp. 155-179, 1985.
- [3] Jan-Reneé Carlson, Langley Research Center, Hampton, Virginia, "Inflow/Outflow Boundary Conditions with Application to FUN3D," October 2011. [Online]. Available: <https://fun3d.larc.nasa.gov/papers/NASA-TM-2011-217181.pdf>.
- [4] Christopher Rumsey, NASA Langley Research Center, "SA Expected Results - 2D Airfoil Near-Wake," 1 March 2023. [Online]. Available: https://turbmodels.larc.nasa.gov/airfoilwakeverif500c_sa.html.
- [5] ANSYS, "4.3.2 Transport Equation for the Spalart-Allmaras Model," 23 January 2009. [Online]. Available: <https://www.ansys.com/doc/api/html/nodes/Node50.htm>.
- [6] ANSYS, "4.3.7 Wall Boundary Conditions," 23 January 2009. [Online]. Available: <https://www.ansys.com/doc/api/html/nodes/Node55.htm>.
- [7] Cadence CFD Solutions, "Y+ Boundary Layer Thickness," 2023. [Online]. Available: <https://resources.system-analysis.cadence.com/blog/msa2023-y-boundary-layer-thickness>.

Appendix A – Hand Calculations for Fluid Stream Variables

Final Project

Verif/2D ANW Near Wake

Model A airfoil @ 0° angle of attack

Reynolds # $R_c = 1.2 \text{ million}$

Upper boundary layer tripped 16% upper surface
lower b.c. tripped 5% lower surface

Mach $M = 0.88$

angle of attack $\approx L = 0$, $T_{ref} = 540^\circ\text{R}$ Ramberg

$$M = \frac{V}{a} = 0.88 \Rightarrow V = a m$$

$$c = \sqrt{\gamma R T}$$

$$T = 540^\circ\text{R} = 300\text{K}$$

$$R = .287 \text{ kJ/kgK}$$

$$\gamma = \frac{C_p}{C_v} = 1.4 \text{ at } 540^\circ\text{R}$$

$$a = \sqrt{(1.4)(.287 \frac{\text{kJ}}{\text{kgK}})(300\text{K})} = 346.58 \text{ m/s}$$

$$V = a m = (346.58)(0.88) = 301.69904 = \underline{\underline{21.7 \text{ m/s}}}$$

$$R_{cL} = \frac{VL}{V} = \frac{V_e}{V} \quad V_e(t, p) = V_e(T=300\text{K}, p=1\text{ atm}) = 1.571 \text{ E}^{-5} \text{ m}^2/\text{s}$$

$$R_{cL} = \frac{(21.7 \frac{\text{m}}{\text{s}})(1\text{m})}{1.571 \text{ E}^{-5} \text{ m}^2/\text{s}} = 1.382 \text{ E} 6 \leftarrow \text{not 1.2, so...}$$

find the proportion

$$R_{cL} = \frac{\rho V c \Rightarrow \rho}{\mu} = \frac{(1.2 \text{ E} 6)(1.857 \text{ E} -6 \frac{\text{m}}{\text{s}^2})}{(21.7 \frac{\text{m}}{\text{s}})(1\text{m})} = \rho \approx \frac{1.023}{1.023}$$

$$\rho = 1.023 \text{ kg/m}^3$$

Appendix B – Modified Airfoil Grid

#Group	#point	#x_coord	#y_coord	#z_coord
1	1	1	0	0
1	2	0.998697154	-8.70375E-05	0
1	3	0.997246115	-0.000184351	0
1	4	0.995630534	-0.000293074	0
1	5	0.993832376	-0.000414436	0
1	6	0.991831781	-0.000549755	0
1	7	0.989606912	-0.000700429	0
1	8	0.987133803	-0.000867902	0
1	9	0.984386208	-0.00105362	0
1	10	0.981335441	-0.001258923	0
1	11	0.977950227	-0.001484843	0
1	12	0.974196548	-0.001731647	0
1	13	0.970037468	-0.001997656	0
1	14	0.965432923	-0.002276681	0
1	15	0.960340206	-0.002565992	0
1	16	0.954714187	-0.002870774	0
1	17	0.948507954	-0.003215537	0
1	18	0.941671663	-0.003618674	0
1	19	0.934151852	-0.004076323	0
1	20	0.92589293	-0.004582836	0
1	21	0.916838416	-0.005142038	0
1	22	0.906931361	-0.005762558	0
1	23	0.896114423	-0.0064452	0
1	24	0.884331306	-0.007189285	0
1	25	0.871528367	-0.007998323	0
1	26	0.857655786	-0.00887555	0
1	27	0.842669208	-0.009823964	0
1	28	0.826531493	-0.01084549	0
1	29	0.809214832	-0.011943803	0
1	30	0.790702639	-0.01312262	0
1	31	0.770991327	-0.014382195	0
1	32	0.75009251	-0.015724042	0
1	33	0.72803453	-0.017148435	0
1	34	0.704863731	-0.018653073	0
1	35	0.680645482	-0.02023491	0
1	36	0.655464488	-0.021889581	0
1	37	0.62942463	-0.023613852	0
1	38	0.602647179	-0.025394413	0
1	39	0.575269194	-0.027210903	0
1	40	0.547441821	-0.029048107	0
1	41	0.51932684	-0.030891638	0
1	42	0.49109188	-0.032710819	0

1	43	0.462908716	-0.034494255	0
1	44	0.434942722	-0.036146521	0
1	45	0.407358556	-0.037639509	0
1	46	0.380307306	-0.03884779	0
1	47	0.353934566	-0.039750839	0
1	48	0.328369624	-0.040268614	0
1	49	0.303728807	-0.040395022	0
1	50	0.280111895	-0.040002367	0
1	51	0.257596598	-0.039273634	0
1	52	0.23623082	-0.038487637	0
1	53	0.216051001	-0.03762252	0
1	54	0.197079964	-0.036594187	0
1	55	0.179322815	-0.035393315	0
1	56	0.162762577	-0.034126217	0
1	57	0.147368906	-0.03288575	0
1	58	0.133106355	-0.031691644	0
1	59	0.119933897	-0.030533239	0
1	60	0.107803381	-0.029411985	0
1	61	0.096662027	-0.028331132	0
1	62	0.086452998	-0.027304617	0
1	63	0.077118528	-0.026338435	0
1	64	0.068601192	-0.025430163	0
1	65	0.060844408	-0.024573939	0
1	66	0.053793292	-0.023759989	0
1	67	0.047395595	-0.022972704	0
1	68	0.041600353	-0.022206151	0
1	69	0.036361285	-0.021440858	0
1	70	0.031636132	-0.020654923	0
1	71	0.027383421	-0.019845179	0
1	72	0.023559407	-0.019035069	0
1	73	0.020130845	-0.018210247	0
1	74	0.01706797	-0.017359209	0
1	75	0.014341852	-0.016482209	0
1	76	0.011924376	-0.015586173	0
1	77	0.009786547	-0.014685358	0
1	78	0.007895328	-0.01380429	0
1	79	0.006238666	-0.012925349	0
1	80	0.004818195	-0.012019005	0
1	81	0.003637134	-0.011072754	0
1	82	0.002690493	-0.010097965	0
1	83	0.001955783	-0.009123824	0
1	84	0.00142004	-0.008168904	0
1	85	0.001041079	-0.007262292	0
1	86	0.000768451	-0.006423955	0

1	87	0.000569433	-0.00565877	0
1	88	0.000422502	-0.004965177	0
1	89	0.000313131	-0.004338922	0
1	90	0.000231298	-0.003774961	0
1	91	0.000169879	-0.003267839	0
1	92	0.000123751	-0.002812353	0
1	93	8.91502E-05	-0.002403513	0
1	94	6.3292E-05	-0.002036782	0
1	95	4.40804E-05	-0.001707902	0
1	96	2.99367E-05	-0.001413091	0
1	97	1.96572E-05	-0.001148872	0
1	98	1.2321E-05	-0.000912097	0
1	99	7.22225E-06	-0.000699947	0
1	100	3.8178E-06	-0.000509896	0
1	101	1.68849E-06	-0.000339651	0
1	102	5.1126E-07	-0.000187154	0
1	103	3.72283E-08	-5.05609E-05	0
1	104	8.67472E-08	7.66923E-05	0
1	105	7.07406E-07	0.00021635	0
1	106	2.15203E-06	0.000372287	0
1	107	4.77615E-06	0.000546395	0
1	108	9.07313E-06	0.00074078	0
1	109	1.57282E-05	0.000957781	0
1	110	2.56915E-05	0.001199944	0
1	111	4.02864E-05	0.001470132	0
1	112	6.13537E-05	0.001771498	0
1	113	9.14366E-05	0.002107332	0
1	114	0.000134062	0.00248133	0
1	115	0.00019402	0.002897081	0
1	116	0.000277786	0.003358395	0
1	117	0.000393783	0.003868533	0
1	118	0.000552607	0.004430168	0
1	119	0.000766887	0.005045072	0
1	120	0.001050574	0.005713734	0
1	121	0.0014179	0.006435736	0
1	122	0.001882288	0.007210513	0
1	123	0.002451587	0.008041251	0
1	124	0.003131074	0.008934755	0
1	125	0.003938932	0.009889771	0
1	126	0.004895358	0.010903254	0
1	127	0.006022006	0.011970719	0
1	128	0.007341639	0.013086257	0
1	129	0.00887807	0.014242897	0
1	130	0.010654582	0.015435158	0

1	131	0.012681692	0.016680622	0
1	132	0.014987058	0.017975614	0
1	133	0.017603131	0.019310837	0
1	134	0.02056144	0.020681616	0
1	135	0.023893428	0.022088608	0
1	136	0.027622535	0.023560843	0
1	137	0.031771023	0.025143389	0
1	138	0.036404736	0.026774906	0
1	139	0.041581398	0.028412995	0
1	140	0.047346666	0.030053994	0
1	141	0.053741433	0.031723359	0
1	142	0.060802476	0.033481132	0
1	143	0.068581046	0.035345488	0
1	144	0.077134539	0.037317175	0
1	145	0.086524444	0.039382845	0
1	146	0.096817342	0.041503274	0
1	147	0.108086102	0.043593319	0
1	148	0.12038946	0.045615997	0
1	149	0.133773202	0.047589019	0
1	150	0.148275453	0.049561653	0
1	151	0.163935573	0.051535372	0
1	152	0.180795291	0.053421153	0
1	153	0.198872539	0.055232613	0
1	154	0.218177025	0.056943844	0
1	155	0.238705211	0.058509855	0
1	156	0.260431099	0.059961102	0
1	157	0.283316696	0.061248776	0
1	158	0.307302011	0.062369079	0
1	159	0.332308289	0.063302014	0
1	160	0.35823876	0.063966247	0
1	161	0.384975037	0.064323445	0
1	162	0.412380396	0.064293401	0
1	163	0.440301089	0.063845099	0
1	164	0.468571475	0.062995335	0
1	165	0.497018136	0.061757629	0
1	166	0.525466312	0.060200565	0
1	167	0.553739311	0.058336236	0
1	168	0.581665579	0.056195019	0
1	169	0.609081979	0.053808143	0
1	170	0.635837277	0.051207257	0
1	171	0.661797531	0.048446314	0
1	172	0.686844674	0.045561717	0
1	173	0.710882626	0.042613573	0
1	174	0.733832076	0.039633298	0

1	175	0.755636523	0.036672483	0
1	176	0.776254185	0.033745901	0
1	177	0.795668557	0.030915644	0
1	178	0.813877254	0.028221935	0
1	179	0.830886518	0.025660571	0
1	180	0.846721282	0.023264869	0
1	181	0.861414161	0.021045791	0
1	182	0.875002782	0.018988284	0
1	183	0.887533512	0.017088897	0
1	184	0.899057667	0.015342621	0
1	185	0.909629975	0.013743553	0
1	186	0.919306809	0.01228267	0
1	187	0.92814503	0.010948274	0
1	188	0.936201944	0.009732511	0
1	189	0.943533706	0.008626315	0
1	190	0.950196399	0.007631032	0
1	191	0.956245249	0.00675698	0
1	192	0.961725813	0.005965469	0
1	193	0.966683108	0.005232687	0
1	194	0.971161634	0.004551497	0
1	195	0.975204273	0.003923556	0
1	196	0.97885108	0.003351006	0
1	197	0.982138568	0.002831794	0
1	198	0.985100206	0.002362487	0
1	199	0.987766678	0.001939229	0
1	200	0.990166072	0.001558126	0
1	201	0.992324051	0.001215413	0
1	202	0.994264021	0.000907533	0
1	203	0.996007286	0.000631175	0
1	204	0.997573211	0.00038328	0
1	205	0.998979364	0.000161044	0
2	1	0.998979364	0.000161044	0
2	2	1	0	0